IASJ المجلات الاكاديمية العراقية

Tikrit Journal of Pure Science

ISSN: 1813 – 1662 (Print) --- E-ISSN: 2415 – 1726 (Online)

Journal Homepage: http://tjps.tu.edu.iq/index.php/j

Study of the Influence of Annealing Temperature on the Structural Properties for ($Ni_{1-x}Zn_xFe_2O_4$) Compounds

Najat A. Dahham , Abdulsamee F. A. Albayati , Inteesar A. Hamed

Department of Physics, College of Science, Tikrit University, Tikrit, Iraq

https://doi.org/10.25130/tjps.v25i3.253

ARTICLE INFO.

Article history:

-Received: 8 / 3 / 2020

-Accepted: 22 / 4 / 2020

-Available online: / / 2020

Keywords: Nikel – Zinc ferrites, chemical precipitation method , XRD,AFM analysis

Corresponding Author:

Name: Inteesar A. Hamed

E-mail:

enteesar.ali1988@yahoo.com

Tel:

ABSTRACT

Nikel-Znic ferrites with chemical formula $Ni_{1-x}Zn_xFe_2O_4$ for (x:0.00 , 0.5 and 1) were synthesis by chemical co-precipitation method at various annealing temperatures (27°C,300°C,600°C,900°C, 1200°C) for (4h). The samples were examined via X-ray diffraction patterns. The XRD pattern confirm the formation of face centered cubic structure (fcc) for all samples. The particle size, lattice parameter, theoretical density and porosity were also measured by X-ray diffraction, and bulk density. It is noted that granular particle size increases with increasing annealing temperature, while decreasing lattice constant, theoretical density and porosity with increasing annealing temperature. The homogeneity, regularity, particle size and the roughness of sample surfaces were calculated using atomic power microscope technique.

1. Introduction

Recently, Nanotechnology becomes at forefront of the most important fields. It has become the subject the interest of many researchers around the world due to the innovative phenomenon, especially the properties presented by nanoparticles, and the ferrites are one of these materials that continue to develop, where they are included in the construction of electrical circuits operating at low or high frequencies[1]. To prepare these materials, including the solid state interactions method and the chemical co-precipitation method that is used in the preparation of nanomaterial's for the ferrite compounds within the frame of this research, if this method was chosen for easy preparation, short time, and not needing high temperatures during preparation[2,3]. In this research, the samples were synthesis by co-precipitation method, and then their structural properties were studied, represented by the lattice constant, porosity and surface topography by X-ray diffraction and atomic force microscopy.

2. Experimental

2-1 Preparation Method

The raw materials used are iron nitrate [Fe(NO3)3.9H2O], zinc nitrate [Zn(NO3)2.6H2O], nickel nitrate [Ni(NO3)2.6H2O],(99% purity) in a different molar ratios. The metals nitrate were weighted by using sensitive Scale (Denver model) with accuracy of 10^{-4}gm, and dissolved separately in 200ml of distilled water by magnetic stirrer for (1.5h) to obtain a perfectly homogeneous solution. Iron was filtered and mixed all the solutions at a temperature of (60C) using magnetic stirrer. To prepare Sodium hydroxide solution(40g) in 200ml of distilled water by continuing magnetic stirrer for (15min) as the precipitating agent. This solution was precipitated with NaOH solution having pH=12 at 60 °C with continuous stirring. The precipitated solutions was washed well, dried in an oven at 100°C for (1h), to get rid of reaction residues like water molecules and obtain ferrites powder. The powder was crushed by using Gate Mortar for (0.5h) an added poly vinyl alcohol(PVA) and mixed well, to obtain the homogenous mixture. The ferrite powder mixture was pressed in to cylindrical pellets of 10 mm diameter by applying hydraulic pressure of 5tons for (1minutes). The pressed samples were sintered at room temperature and different annealing temperatures range from(300°C to 1200°C) for (4h).The samples are left inside the oven to be cooled slowly to room temperature. The prepared samples $NiFe_2O_4$,$ZnFe_2O_4$ and $Ni_{0.5}Zn_{0.5}Fe_2O_4$ were named A, B and C, respectively.

2.2 Characterization

The X-ray diffraction patterns of the sample was identified using X-ray Diffractometer (XRD-6000 from SHIMADZU) using Cu Kα radiation (λ =

1.5406 Å), using (2θ) = 10°- 80° in steps of 5deg/s. Atomic Force Microscope AFM (AA3000 from Angstrom Advanced Inc. German.) was used to study the topography of surface, surface roughness, average square root and grain size of all samples.

3. Results and Discussion

3-1 XRD Results

X-Ray Diffraction (XRD) was used to analysis the crystal structure and the structural properties of annealed samples.It was observed that all samples are of a normal spinal ferrite phase and have a cubic-center structure (FCC) as shown in Fig (1) which prepared at room temperature and different annealing temperatures. Miller's indices were set on represented (220), (311), (222), (400), (511), (440), (533), as they appeared match with ICDD cards (00-054-0964, 00-022-1012, 00-052-0278), this results that agreed by a lot of researchers[4-6] . For of the sample prepared and annealing at different temperatures, it was noticed that when the temperature increased, the peak of the reflections became sharp. This indicates an improvement in the crystal when the annealing temperature increases. Additionally, it is noticed that as the annealing temperature increases, the width of the central maxima decreases. This is due to the grain size increase with an increase in the annealing temperature.

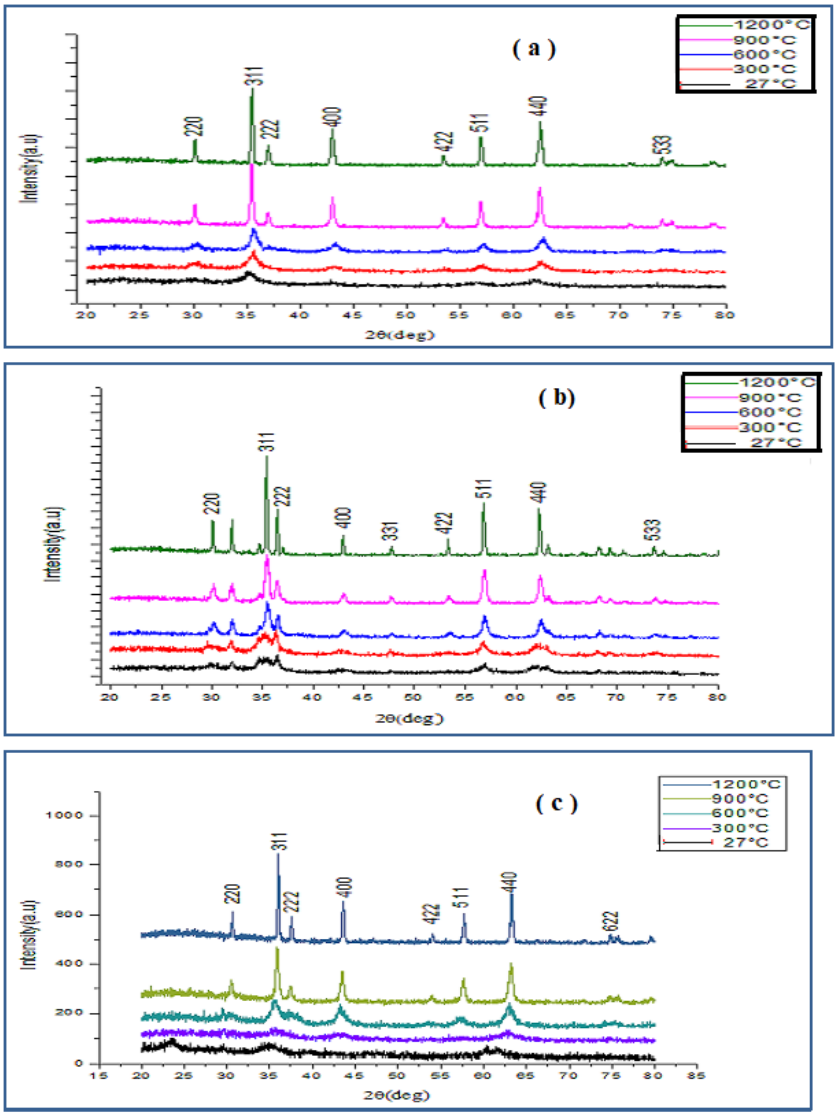

Fig. 1: XRD pattern of (a)A ($NiFe_2O_4$) (b) B ($ZnFe_2O_4$) (c) C ($ZnFe_2O_4$)

Lattice constant for all samples were calculated using the following mathematical relationship [7]:

$a- = d(h^2 + k^2 + l^2)^{1/2}$ ……..(1)

Where (**a**) is lattice parameter, and (hkl) is Miller index.

The particle size (D) was calculated from the following Debye-Scherrer relationship [8]:

$D = 0.9\lambda/\beta \cos\theta$ …..(2)

Where : (λ) is the wavelength of the radiation, (0.15406 nm for Cu Kα), (θ) is the Bragg's angle . Full width at half maximum (FWHM).

The theoretical density(ρ_{x-ray}) and bulk density(ρ_d)was calculated according to the following mathematical relationships[9,10]

$$\rho_{x-ray} = \frac{ZM_{wt}}{VN_a} \quad .....(3)$$

$$\rho_d = \frac{m}{V} \quad .....(4)$$

Where Z is the number of atom per unit cell, M_{wt} is the molar mass of the sample, N_A is the Avogadro's number (6.022 x10^{23}) and V is the volume of the unit cell. m is the mass .

The porosity was calculated based on the theoretical and bulk density according to the mathematical relationship[11]:

$$P = 1 - \frac{\rho_d}{\rho_{x-ray}} \times 100\% \quad .....(5)$$

Table (1) indicates the effect of different annealing temperatures on the structural properties represented by the lattice constant and the theoretical and bulk density at different annealing temperatures.

Table 1: The effect of different annealing temperatures on the structural properties

Sample	Temperature	Lattice Constant(a)	$\rho_{x\text{-ray}}$ (g/cm^3)	ρ_d (g/cm^3)	particle size D nm	Porosity %
A	Rt	8.43	5.2	1.15	6.57	77.88
	300	8.36	5.32	1.17	7.42	77.63
	600	8.33	5.38	1.23	10.73	77.18
	900	8.38	5.29	1.54	29.38	70.89
	1200	8.38	5.29	1.71	32.04	67.67
B	Rt	8.17	5.87	1.03	7.95	82.45
	300	8.19	5.83	1.07	8.39	81.65
	600	8.37	5.46	1.13	14.82	79.3
	900	8.39	5.42	1.37	18.19	74.72
	1200	8.39	5.42	1.79	49.56	66.97
C	Rt	8.49	5.16	0.94	4.1	83.39
	300	8.32	5.48	0.97	13.05	82.3
	600	8.33	5.46	0.99	17.2	81.87
	900	8.29	5.54	1.06	18.96	80.86
	1200	8.26	5.6	1.38	43.06	75.36

3-2 particle size

Figure (2) indicates that annealing temperatures as a function of the particle size, as it turns out that an increase in temperature leads to an increase in the particle size, as a result of the spread of small particles within large particles and the disappearance of grain boundaries between the contact particles. As temperature continues to increase, it turns into larger particles and eliminates existing pores, and this is agree with [5,12,13].

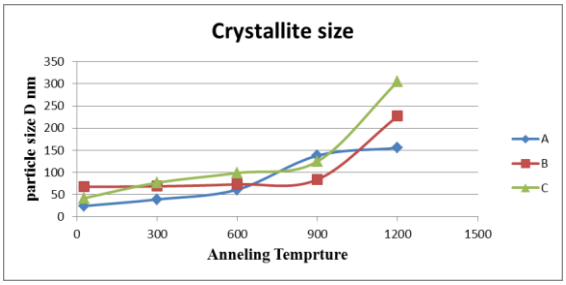

Fig.2: show the variation of grain size with different annealing temperatures

3-3 Lattice Constants

Figure (3) cleared the effect of annealing temperatures on the Lattice constant for all samples. As turns out that increasing the temperature leads to an increase in the crystallization of the material, Hence this will lead to a decrease in the lattice constants of all compounds A, We observed a decrease in the lattice constant of compound C at temperatures 900-1200 °C, due to the cation redistribution between the tetrahedral(A) sites and octahedral (B) sites (increase in the lattice constant), or the loss of zinc from the samples (The value of the lattice constant is low). This is what the researchers agreed [14,15]. The increase of the lattice constant of compound B with annealing temperature, due to the reason that the atomic radii of zinc (0.74A°) are greater than the atomic radius of iron (0.67A°), since the chemical formula indicates that the zinc (Zn^{+2}) is replaced by Fe (Fe^{+3}), this in turn leads to the expansion of the lattice and therefore the lattice constant value increasing [16],or due to the inverse transitions of the positive ions as a result of the temperature rise. These transfers lead to a theoretical density drop because they depend on the lattice constant [17].

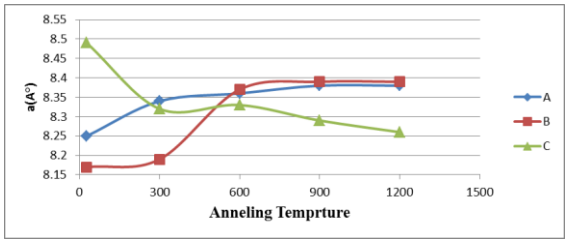

Fig.3: lattice constant as a function of different annealing temperatures

3-4 Theoretical & Bulk Density

Figures (4,5) shown the Influence of annealing temperatures on the properties of theoretical, Bulk density. As it reveals that the increase in temperature leads to an increase in the an Bulk density values, the reason for this is due to the spread of the compound

atoms and the occurrence of the crystal growth process, and also the zinc atomic mass (65.38 amu) and nickel (58.71 amu) are greater than the atomic mass of iron (55.845 amu), As the increase in the element's atomic weight leads to an increase in the bulk density, while the theoretical density values were the highest value for compound A at temperature (600 C°) and compound B at room temperature (RT) while compound C was at temperature(1200C°), this due to the fact that the density by diffraction of X-rays depends on the molecular weight and the lattice constant, and this consistent with relationship (3) that shows the density extraction shown in Table (1). the reason of the theoretical density calculated from the diffraction of X-rays for each sample is greater than the bulk density, it is because of the presence of porosity in the samples, and that these results are agree with previous studies[16].

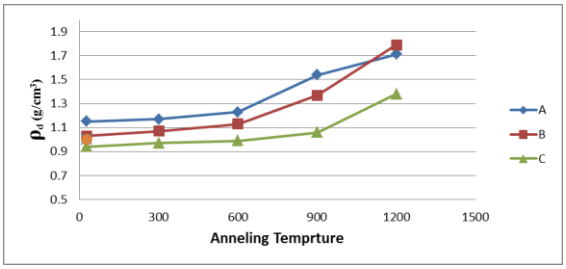

Fig.4. variation Bulk Density as a function of different annealing temperatures for compounds A, B and C

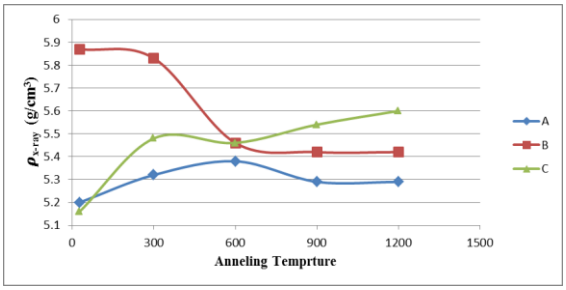

Fig.5. variation theoretical Density as a function of different annealing temperatures for compounds A, B and C

3-5 Porosity

Figure (6), it is clear the effect of annealing temperatures on the Porosity for the samples, whereas the porosity decreases with annealing temperatures increasing , because of the formation of positive ions (cations) and fewer oxygen vacancies[18].

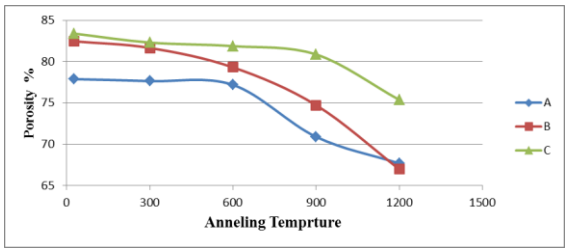

Fig. 6: variation Porosity as a function of different annealing temperatures for compounds A, B and C

4. Atomic Force Microscope Results

The Atomic force Microscope(AFM) showed that results of the surface topography, represented on the values of surface roughness and average square root, also the grain size of selected models at room temperature and different annealing temperatures were determined . Figs(7-12) which shows images of the two-dimensional, three dimensional and distribution of the grains respectively.

It has been observed that the average surface roughness and the average square root decreases with increasing temperature, while average grains size increases as shown in Table (2). As Turn out that the increase in temperature contributes to increasing the grain size, due to the regular crystal homogeneity and crystal growth horizontally above the surface, This reduces the surface defects for all samples, This improves the mechanical and magnetic properties, and this is correspond with the results of the theoretical density and porosity calculated by X-ray diffraction.

Among the figures shown, the distribution of granular groups grown on the surfaces of the models increases and decreases with increasing temperature, and it was observed that the grain size measured with AFM technique is greater than the grain size measured by XRD technique, because AFM measures on the surface of the model, while XRD technology measures inside the model. [19].

Table 2: Values obtained from AFM analysis.

temperature	Roughness Average (nm)	Root mean Square (nm)	Grain size (nm)
Rt	6.74	8.09	73.22
600	1.58	2.01	90.59
1200	1.37	1.73	93.98
Rt	6.64	8.0	85.06
600	2.79	3.48	93.35
1200	2.42	3.02	123.64
Rt	4.55	5.69	75.20
600	4.24	5.25	90.73
1200	2.62	3.50	113.43

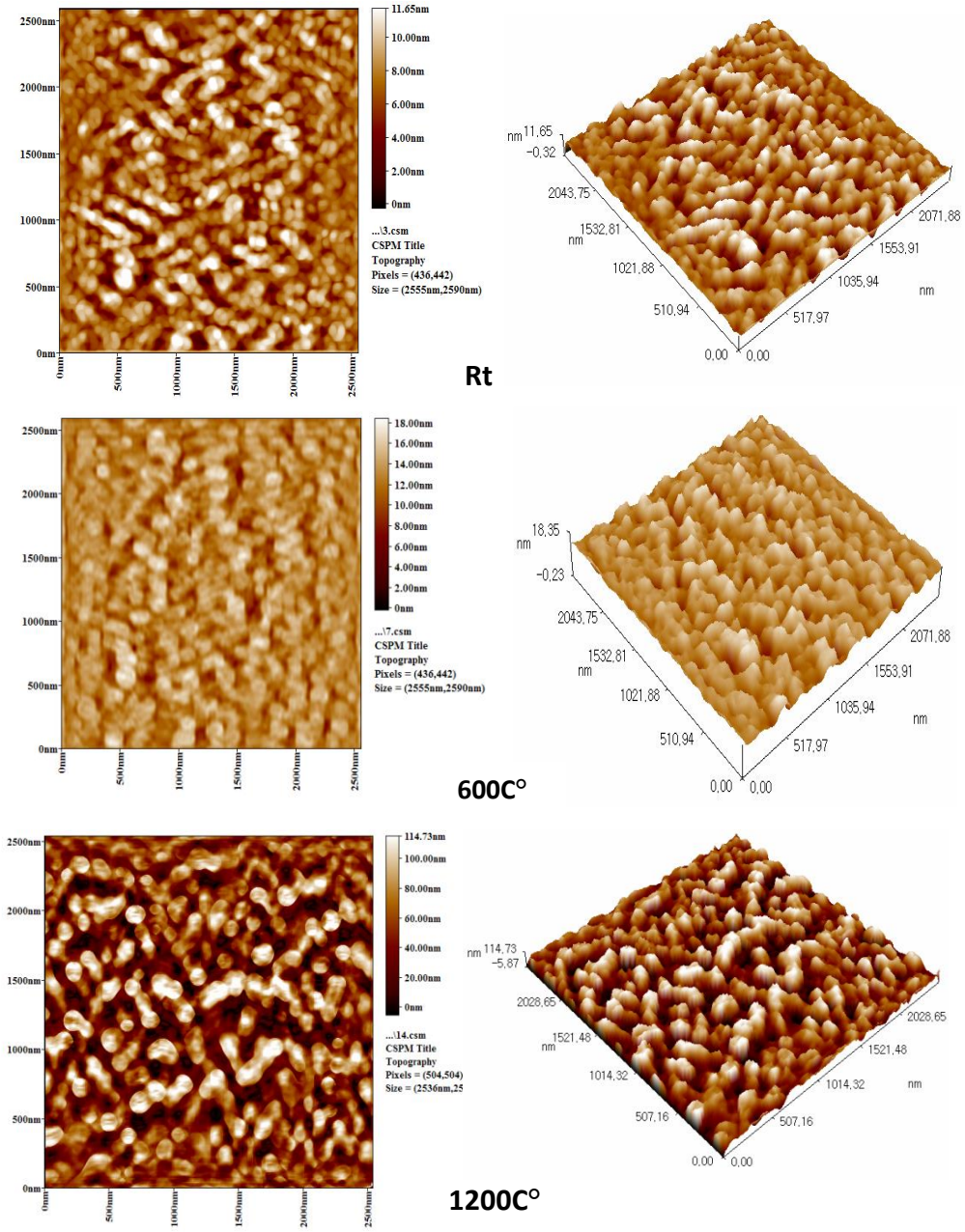

Fig. 7: AFM images of A Compounds in (2D-3D) dimensional .

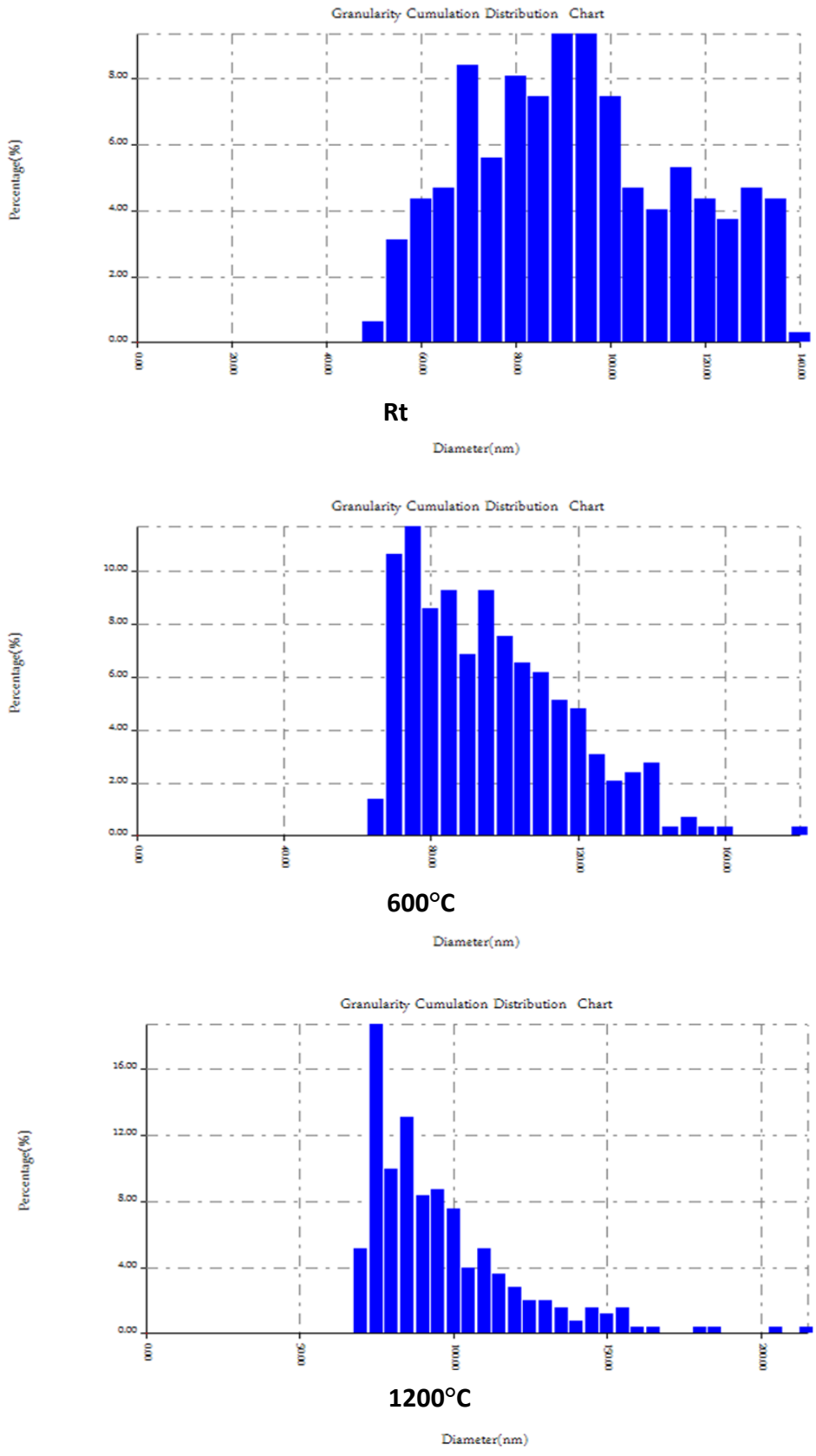

Fig. 8: Particle size distribution of A Compounds

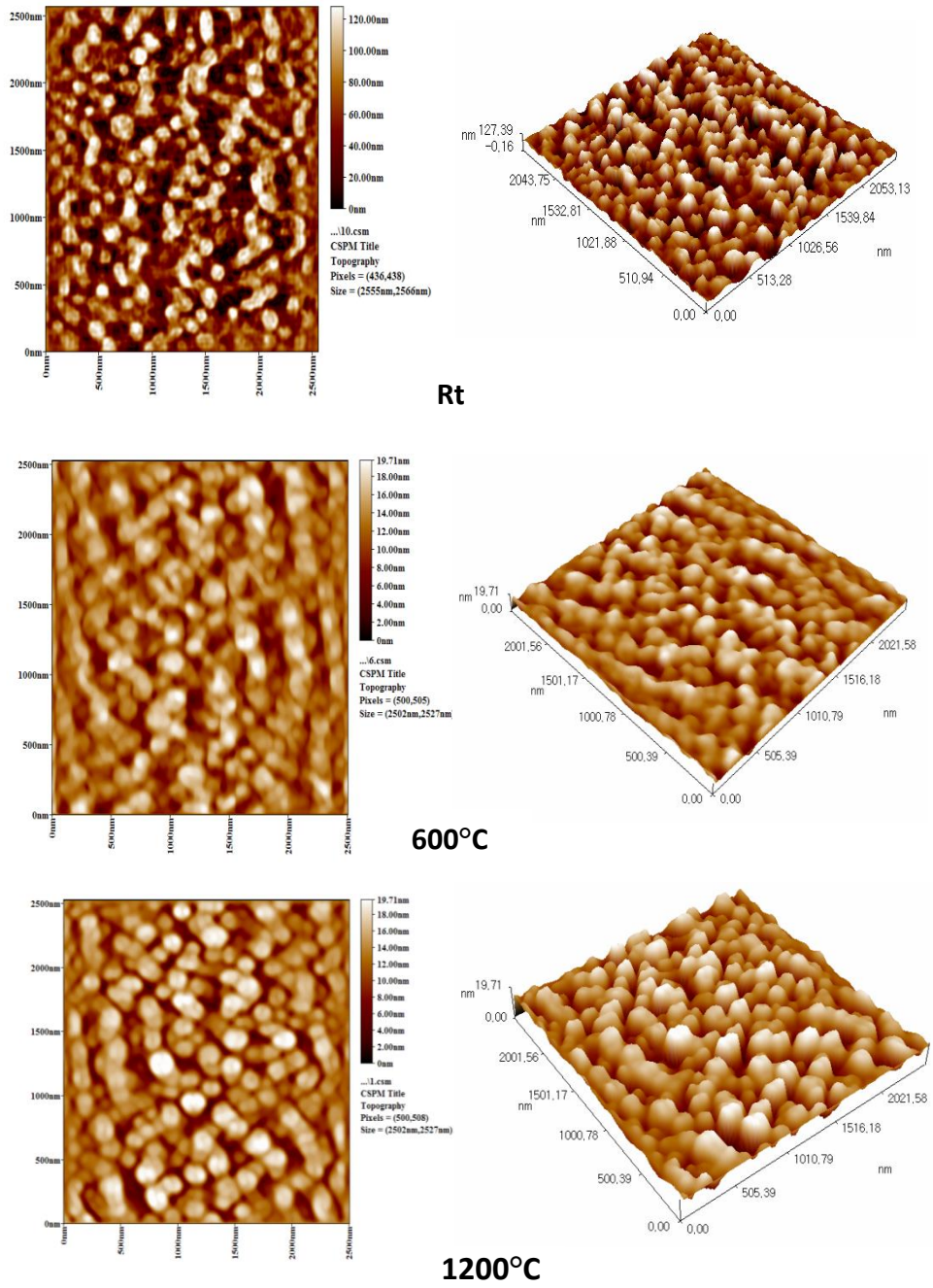

Fig. 9. AFM images of B in (2D-3D) dimensional

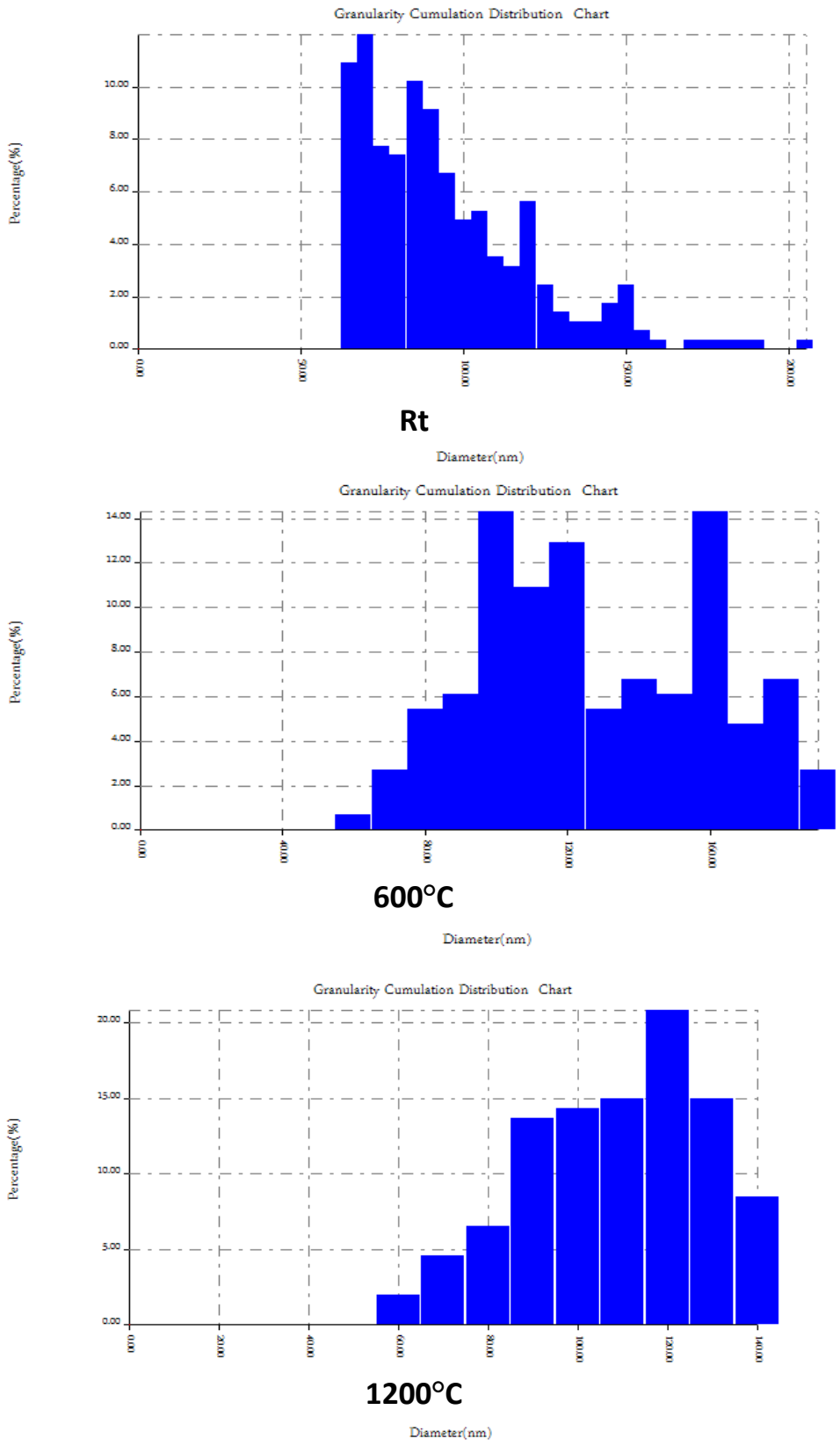

Fig. 10: Particle size distribution of B Compounds .

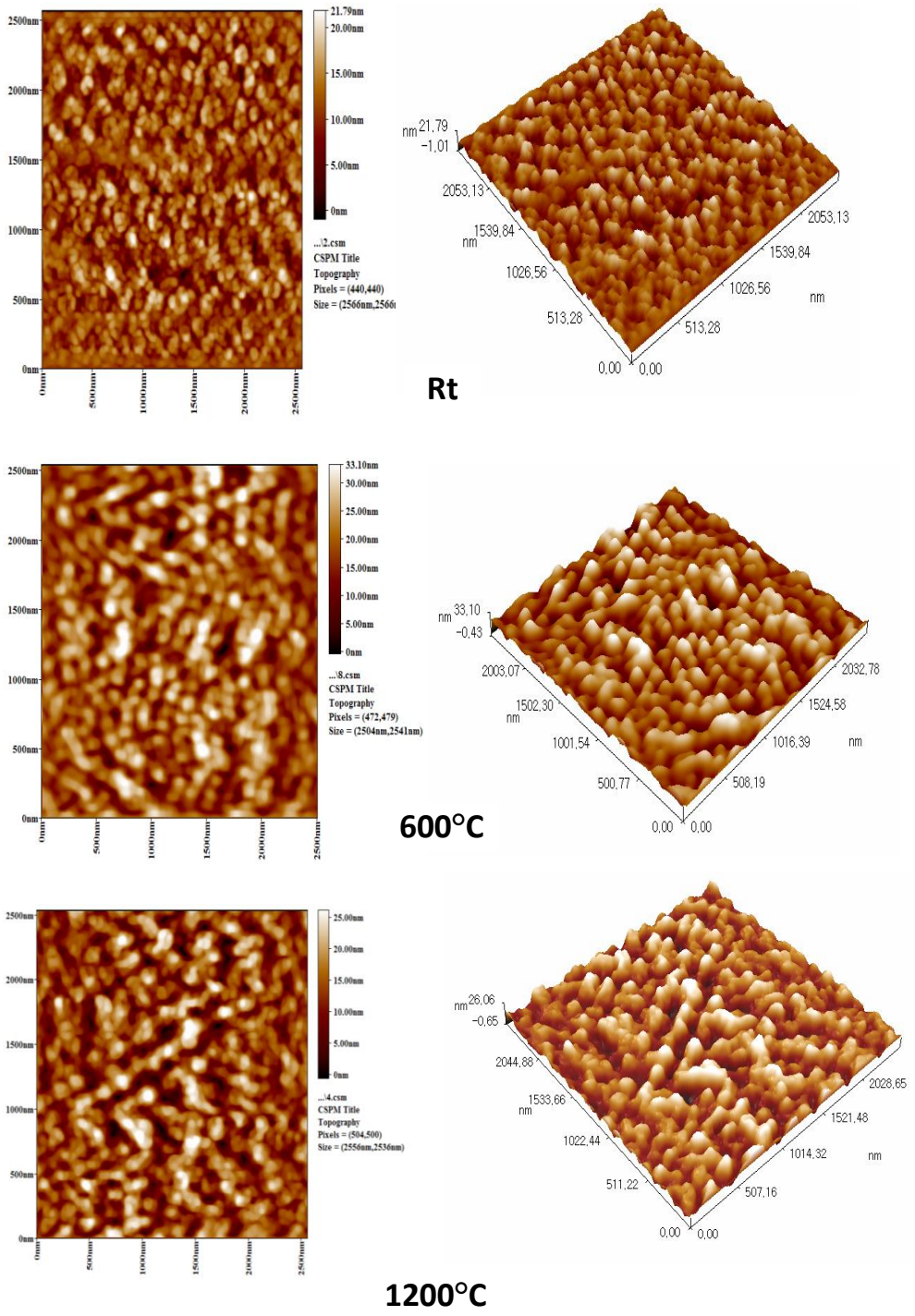

Fig. 11. AFM images of C Compounds in (2D-3D) dimensional

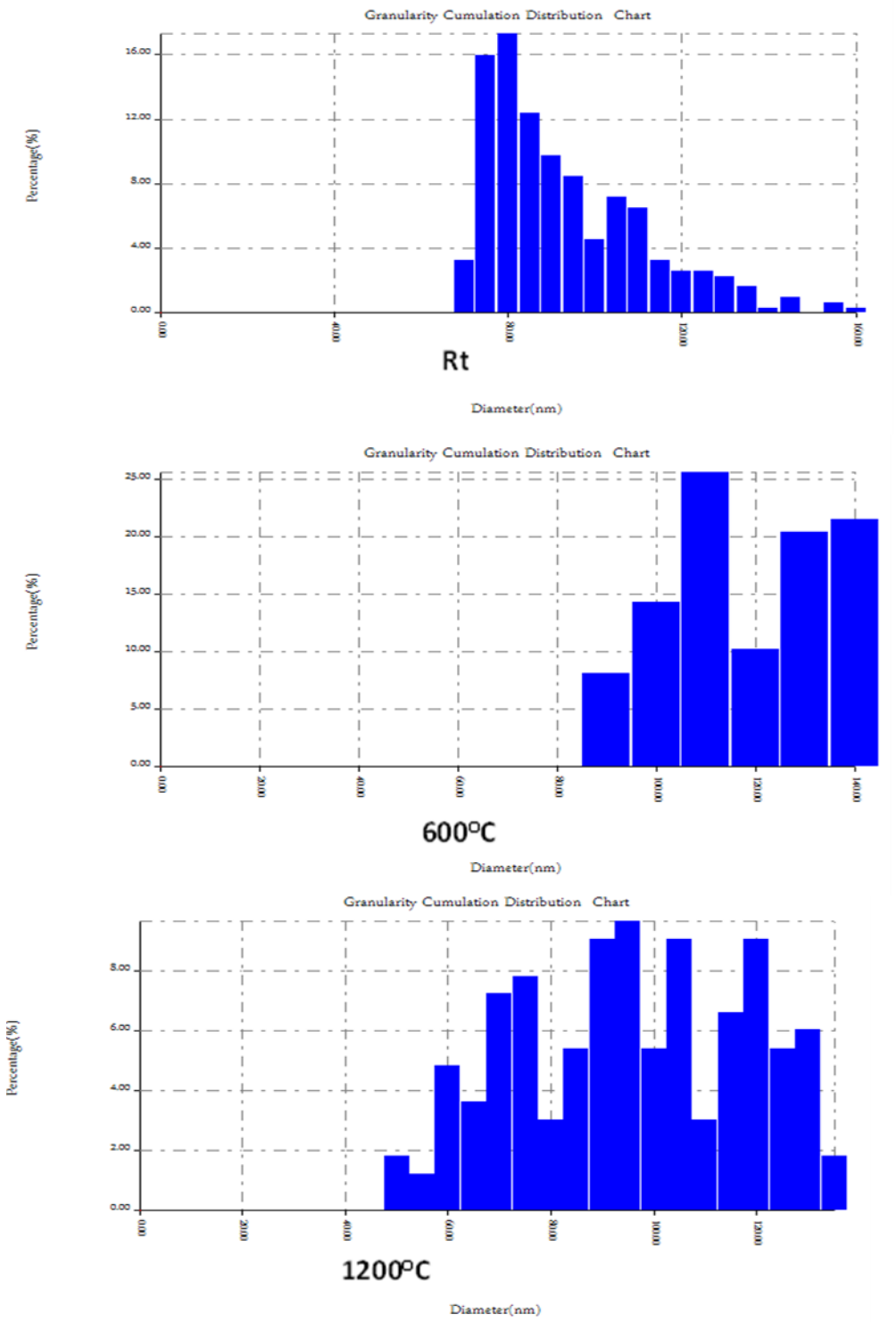

Fig. 12: Particle size distribution of C sample

References

[1] Bowen, H.K.; Human, D.R. and Gingery, W. (1976).Introduction to ceramics. 2nd edn. John Wiley and Sons , New York.

[2] Dunlap, R. A.; Alghamdi, A.; O'Brien, J. W.and Penney, S. J. (2004). A Mössbauer effect investigation of superparamagnetic behavior in ball milled Mn–Zn ferrites. *Journal of Alloys and Compounds*, **365(1)**: 84-88.

[3] Allouche, J. (2013). Synthesis of Organic and Bioorganic Nanoparticles : An Overview of the Preparation Methods. *Nanomaterials: a danger or a promise*, Springer-Verlag London:27-74pp.

[4] Banerjee, M.;Verma, N. and Prasad, R. (2007). Structural and catalytic properties of Zn_{1-x} Cu_xFe $_2O_4$ nanoparticles. *Journal of materials science,* **42(5):**1833-1837.

[5] Jacob, J.; Khadar, M. A.; Lonappan, A.and Mathew, K. (2008). Microwave dielectric properties of nanostructured nickel ferrite. *Bulletin of Materials Science,* **31(6)**: 847-851.

[6] Batoo, K. M.and Ansari, M. S. (2012). Low temperature - fired Ni-Cu-Zn ferrite nanoparticles through auto-combustion method for multilayer chip inductor applications. *Nanoscale research letters*, **7(1)**: 112.
[7] Shinde, T. J.; Gadkari, A. B.and Vasambekar, P. N. (2008). DC resistivity of Ni–Zn ferrites prepared by oxalate precipitation method. *Materials Chemistry and Physics*, **111(1)**: 87-91.
[8] Cullity, B. D. (1978). Elements of x-ray diffraction. Reading, MA: Addison - Wesley Publishing Company, Inc.
[9] Sultan, N. T. (2011). Increased Porosity and Their Effect on The Density and Hardness Value of (Ni—Cu) Alloy. *Engineering and Technology Journal*, **29(1)**:66-74.
[10] Kurian, M. and Nair, D. S. (2016). Effect of preparation conditions on Nickel Zinc Ferrite nanoparticles: A comparison between sol–gel auto combustion and co-precipitation methods. *Journal of Saudi Chemical Society*, **20(1)**:S517-S522.
[11] Suresh, S. (2013). Synthesis, structural and dielectric properties of zinc sulfide nanoparticles. *International Journal of Physical Sciences*, **8(21):**1121-1127.
[12] Sileo, E. E.; Rotelo, R. and Jacobo, S. E. (2002). Nickel zinc ferrites prepared by the citrate precursor method. *Physica B: Condensed Matter*, **320(1-4):** 257-260.
[13] Zi, Z. et.al. (2013). Size Effects on Magnetic Properties of $Ni_{0.5}Zn_{0.5}$ Fe_2O_4 Prepared by Sol-Gel Method. *Advances in Materials Science and Engineering*,**2013**:1-10.
[14] Sutka, A.; Gross, K. A.; Mezinskis, G.; Bebris, G. and Knite, M. (2011). The effect of heating conditions on the properties of nano - and microstructured Ni–Zn ferrite. *Physica Scripta*, **83(2)**:025601.
[15] Ognjanović, M. et.al. (2019). Bifunctional (Zn,Fe)3O4 nanoparticles: Tuning their efficiency for potential application in reagentless glucose biosensors and magnetic hyperthermia. *Journal of Alloys and Compounds*,**777**: 454-462.
[16] Bera, J. and Roy, P. K. (2005). Effect of grain size on electromagnetic properties of $Ni_{0.7}Zn_{0.3}Fe_2O_4$ ferrite. *Physica B: Condensed Matter*, **363(1)**: 128-132.
[17] Jawad, N.A. (2018). Study of Some Physical Properties for Nano Chemically Prepared Compound of ($Zn_xFe_{x-3}O_4$), M.Sc. thesis, Tikrit University, Tikrit, Iraq.
[18] Paramesh, D.; Kumar, K. and Reddy, P. (2016). Influence of nickel addition on structural and magnetic properties of aluminium substituted Ni-Zn ferrite nanoparticles. *Processing and Application of Ceramics*, **10(3)**:161-167.
[19] Babu, K.V.; Chandra, M. R.; Kumar, G. V. S. and Jagadeesh, K. (2017). Effect of cobalt substitution on structural, electrical and magnetic properties of NiFe2O4. *Processing and Application of Ceramics*,**11(1):**60-66.

دراسة تأثير درجات حرارة التلدين على الخواص التركيبية للمركب($Ni_{1-x}Zn_xFe_2O_4$)

نجاة احمد دحام ، عبد السميع فوزي عبد العزيز ، انتصار علي حميد

قسم الفيزياء ، كلية العلوم ، جامعة تكريت ، تكريت ، العراق

الملخص

تم تحضير مركبات الفرايت ذات الصيغة الكيميائية ($Ni_{1-x}Zn_xFe_2O_4$) باستخدام تقنية الترسيب الكيميائي عند درجات حرارة تلدين مختلفة (27,300,600,900 and1200°C) ولمدة(4h) وبنسب وزنية(x=0, 0.5 and 1) ، كما تم فحص العينات بدلالة تقنية حيود الاشعة السينية للتاكد من تشكيل الطور المغزلي الاعتيادي (spinal ferrite) ذو تركيب مكعب متمركز الاوجه (FCC) لجميع النماذج، كما تم حساب الحجم الحبيبي وثابت الشبيكة والكثافة الظاهرية والمسامية من حيود الاشعة السينية، والكثافة الفيزياوية ، إذ لوحظ ان الحجم الحبيبي يزداد مع زيادة درجة الحرارة ، بينما يتناقص كل من ثابت الشبيكة والمسامية والكثافة الفيزيائية بزيادة درجة حرارة التلدين ،اما تجانس وانتظام سطوح العينات وحساب الحجم الحبيبي ومدى خشونة السطح فقد تم دراسته بدلالة تقنية مجهر القوى الذرية.